RSC Advances

PAPER

View Article Online
View Journal | View Issue

Cite this: *RSC Adv.*, 2020, **10**, 23607

Digital light processing 3D printing of modified liquid isoprene rubber using thiol-click chemistry†

Lara Strohmeier, Heike Frommwald and Sandra Schlögl *

Received 10th May 2020
Accepted 15th June 2020

DOI: 10.1039/d0ra04186f

rsc.li/rsc-advances

This study highlights the additive manufacturing of diene-rubbers with digital light processing (DLP). The network formation relies on the crosslinking of a methacrylate-functional liquid isoprene rubber *via* photo-induced thiol-click chemistry. Bi-functional divinyl ethers are added as reactive diluents, which benefit from a low potential for skin irradiation and skin sensitization. Along with significantly reducing the viscosity, the divinyl ethers accelerate the cure kinetics of the diene-rubber across the main chain C=C bonds of the isoprene units. Photo-DSC measurements reveal that the length of the glycol-spacer and the chemical structure (glycol *versus* alkyl) of the divinyl ether influence the photo-reactivity of the rubber formulations in thiol–ene reactions. In the present study, the highest reactivity is observed for tri(ethylene glycol) divinylether comprising a spacer with three glycol units. To improve the storage stability of the rubber formulation, a radical scavenger is applied to reduce premature crosslinking reactions under dark conditions. With the stabilized liquid rubber formulations, precise 3D structures with features of 0.5 mm are successfully manufactured with bottom-up DLP 3D printing.

Introduction

Benefiting from unique material properties such as high elasticity, resilience, and excellent electrical and thermal insulation, elastomers are applied in numerous industrial fields (*e.g.* transportation, electronics and energy).[1] With the advent of soft robots[2] and (self)adaptive polymer devices, the interest in 3D-printable elastomers has been steadily growing as their soft and deformable material properties enable safe and smooth interactions with humans whilst their large deformations allow for a wide range of active motions.[3] Conventional additive manufacturing techniques (AMT) for elastomers rely on either selective laser sintering (SLS) and fused filament fabrication (FFF) of thermoplastic elastomers and thermoplastic polyurethanes or direct ink writing methods that are predominately applied for the printing of silicon rubbers.[4,5] The inks contain vinyl-functional siloxane monomers/oligomers, which are crosslinked with a silane through a metal-catalysed hydrosilylation reaction.[6] Moreover, photocurable silicone rubber formulations have been developed and are commercially available (ACEO®);[7] they are printed using the so called drop-on-demand method. With this technique, the print head deposits single resin droplets on a building platform which merge into a homogeneous layer. Between the depositions of each layer, the resin is cured through UV exposure. However, the thermal as well as the photocuring process requires the printed object to be post-cured.[5] In addition, those techniques suffer from poor lateral resolution (determined by the size of the printing nozzle, which is at a hundreds micrometer scale), and the requirement of support materials in the case of printing overhanging structures. This constrains the complexity of macroscopic polymer structures that can be obtained.

For well-established AMTs based on UV curing processes (*e.g.* digital light processing, DLP, stereolithography, SLA and PolyJet), only a few photocurable elastomers are commercially available, including Carbon EPU 40,[8] Stratasys TangoPlus,[9] Formlabs Flexible,[10] and Spot-A Elastic.[11] Those elastomers are based on UV curable urethane acrylates and acrylates with flexible chains that provide the "soft domains" in the cured elastomer networks. By optimizing the composition of the urethane and acrylate monomers, researchers were able to fabricate 3D printed elastomer objects with an elongation of up to 1000%.[12]

Among the printing processes using light to build the object, DLP offers distinctive advantages since it provides high resolution and surface quality at low cost and comparably high throughput rates.[13] It relies on a localized photopolymerization process which is initiated by light in the UV-vis region. The printing is carried out in a vat containing liquid monomers or oligomers and an appropriate photoinitiator.[14] The resin formulation is selectively crosslinked layer-by-layer upon light exposure (Fig. 1b). In contrast to SLA, each layer is illuminated all at once using a selectively masked light source comprising binary patterns (information on each layer is provided in the form of black and white images) presented by a digital micro-

Polymer Competence Center Leoben, 8700 Leoben, Austria. E-mail: sandra.schloegl@pccl.at

† Electronic supplementary information (ESI) available: FTIR spectra of **LIR-REF** and cure kinetics of stabilized and non-stabilized rubber formulations. See DOI: 10.1039/d0ra04186f

mirror device. Thus, the build time is significantly shorter compared to SLA.

Whilst the DLP printing with urethanes has been successfully employed in the fabrication of stretchable objects, the DLP printing with diene-rubber materials is still in its infancy.[15] Due to their salient features including high elasticity, strength, and recovery, diene-rubbers are applied in numerous technical applications.[16] Along with classical sulfur and peroxide curing, several photochemical routes have been established to crosslink diene-rubbers over the past years.[17,18]

One of the most popular reaction mechanisms, is thiol–ene click chemistry, which enables the photo-induced crosslinking of diene-rubbers across their unsaturated carbon double bonds located either in the main or side chain.[17,19,20] Further approaches involve the introduction of functional groups or chromophores into the rubber chains, which undergo crosslinking reactions upon UV exposure.[21] In particular, acrylate or methacrylate groups are often exploited since they are well known for their high reactivity in radical induced chain growth reactions.[22] Thus, diene-rubbers with functional acrylate groups undergo rapid crosslinking upon UV irradiation in the presence of an appropriate photoinitiator.[23,24]

For the DLP printing of diene-rubbers, liquid rubber formulations are required that provide a high photo-reactivity and a low viscosity to fabricate 3D objects with adequate resolution and printing speed. Recently, Scott and co-workers demonstrated the successful printing of a hydrogenated butadiene rubber.[19] The photo-reactivity was obtained by functionalizing the liquid rubber with acrylate-groups. In addition, low-viscous acrylates were added as reactive diluents to increase the cure rate and to reduce the viscosity of the printing formulations.

In a similar approach, Nanni *et al.* used thiol-acrylate chemistry to print an acrylate-functionalized liquid butadiene rubber *via* a layer-by-layer deposition of liquid filaments with a syringe followed by a UV induced curing of each layer.[20] However, due to the limitations of the printing technique, the printed objects were characterized by a rather poor resolution and surface quality.

Inspired by this work, we exploit the concept of thiol-click chemistry for the DLP 3D printing of liquid isoprene rubber. In particular, a commercially available liquid isoprene rubber with methacrylate side chains was used as base resin. Since acrylates and methacrylates are well known for their cytotoxicity and high irritancy potential, which limits their overall biocompatibility, we tried to keep the number of methacrylate functions in the formulation as low as possible.[25] Thus, multifunctional divinyl ethers were used as reactive diluents, which undergo a photo-induced thiol–ene reaction across the carbon double bonds of the isoprene units (Fig. 1a). By optimizing type and concentration of the divinyl ether, DLP 3D printable resin formulations are obtained that are characterized by high curing rates and adequate printing quality.

Results and discussion

Viscosity and storage stability of DLP 3D printable liquid rubber formulations

A low viscosity of the resin plays an important role for the DLP 3D printing process. On the one hand it is related to a higher mobility of the monomers, which facilitates a higher conversion and reactivity in the photo-curing process.[26] On the other hand, a good movability of the resin ensures that it moves quickly to the print area between the depositions of each layer. Thus, the viscosity of common DLP printable resins is typically within the range of 0.25 and 5 Pa s.[27] However, without the addition of diluents, most commercially available liquid rubbers exceed this viscosity range.

For the pure methacrylate-functional liquid isoprene rubber used in the present study, a viscosity of 79 Pa s was determined at room temperature. To decrease the viscosity towards a processible level, selected divinyl ethers (Fig. 1a) were added to the liquid rubber. In addition, a multi-functional thiol and phenylbis(2,4,6-trimethylbenzoyl)phosphine oxide as well as ethyl(2,4,6-trimethylbenzoyl)phenylphosphinate were applied as long-wavelength absorbing photoinitators to cure the rubber formulation by photo-induced thiol–ene chemistry.

It should be noted that thiol–ene systems often suffer from premature polymerization due to a base-induced Michael addition of the thiol groups to the carbon double bonds of the "ene". Furthermore, dark polymerization reactions can be initiated by hydroperoxide impurities or the generation of radicals through a ground-state charge.[28]

To determine the shelf-life of the rubber formulations, their viscosity was monitored under accelerated ageing conditions (50 °C for 24 h) (Fig. 2a). Independent on the type of reactive diluent, the viscosity of the rubber formulations significantly

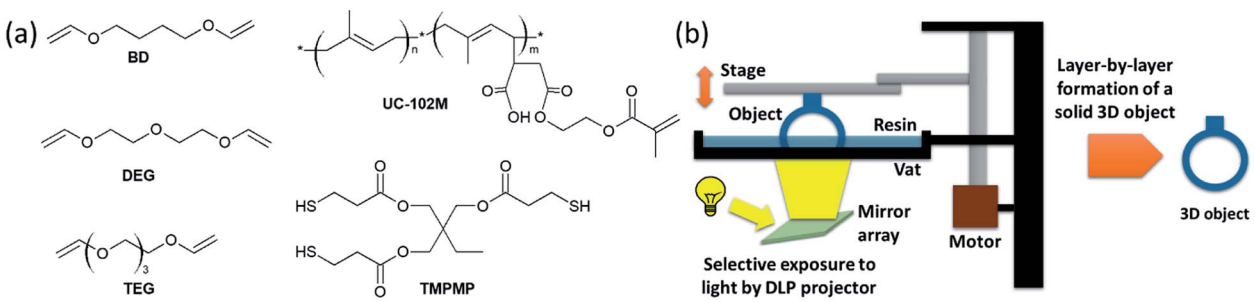

Fig. 1 (a) Reactive diluents, thiol crosslinker and liquid rubber used for the preparation of the 3D printable rubber formulations and (b) DLP 3D printing process for the additive manufacturing of the liquid rubber formulations.

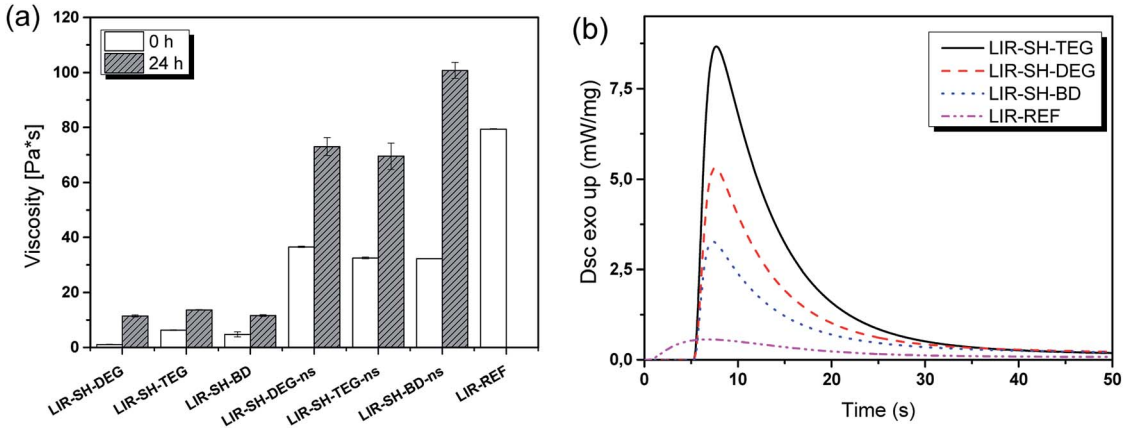

Fig. 2 (a) Influence of the stabilizing agent (0.1 wt% pyrogallol) on the storage stability of the rubber formulations at 50 °C. The term "ns" denotes the formulations without stabilizer. (b) Photo-DSC curves of stabilized rubber formulations.

increased and with 101 Pa s **LIR-SH-BD-ns** even exceeded the initial viscosity of the pure liquid rubber.

To overcome the premature gelation of the rubber formulations, an emphasis was put on finding suitable stabilizer systems. Pyrogallol has been reported as one of the most efficient radical scavengers for thiol–ene systems due to its high resonance stabilization.[29] However, the amount of pyrogallol has to be carefully chosen since the photo-reactivity will decrease upon the addition of radical stabilizers.[30,31]

Directly after mixing, the stabilized formulations comprised a viscosity between 1 and 6 Pa s, which is significantly lower than the viscosity of the non-stabilized ones (11–14 Pa s). The results clearly show that the non-stabilized samples start polymerizing immediately after preparation, which results in resin viscosities beyond the desired processing range. Although the viscosity of the stabilized formulations increased to 32–37 Pa s after prolonged storage at 50 °C, the shelf-life of the formulation at room temperature is sufficiently high for using them in the subsequent DLP 3D printing process.

In this context, it has to be considered that a sufficient storage stability for thiol–ene systems over weeks was only reported for synergistic stabilizer systems, which hinder both, the radical and basic induced dark reactions.[30,31] However, optimizing the shelf-life of the rubber formulations was beyond the scope of this study.

Photo-reactivity and cure kinetics of DLP 3D printable liquid rubber formulations

Along with a low viscosity, resins for DLP 3D printing should show a high monomer conversion after a short period of UV-exposure to make a layer-by-layer build-up of 3D objects feasible. Thus, photo-DSC measurements were performed to determine photo-reactivity and monomer conversion of the stabilized formulations. The released heat of the photo-polymerization corresponds to the peak height of the heat flow of polymerization, whereas t_{max} refers to the time needed to reach the maximum heat flow. Both parameters give insight into the curing speed of the resin. The area is determined by integration of the curve and is attributed to the reaction enthalpy. With this parameter the monomer conversion could be calculated if the theoretical enthalpy of reaction is known. However, this is not applicable for a thiol–ene reaction with vinyl ether groups (from the reactive diluents) and methacrylate functions (from the functionalized liquid rubber) due to the competition between the thiol–ene step-growth reaction and the chain-growth reaction of the methacrylates.[32] The obtained values for the liquid rubber formulations under investigation are displayed in Table 1.

Table 1 Photo-DSC data of stabilized rubber formulations

Formulation	Peak height (mW mg^{-1})	Area (J g^{-1})	t_{max} (s)
LIR-REF	0.6	10.8	7.6
LIR-SH-TEG	8.7	82.3	7.7
LIR-SH-DEG	5.3	58.1	7.6
LIR-SH-BD	3.3	47.3	7.3

In the absence of any reactive diluent and thiol crosslinker, the methacrylate-functional isoprene rubber (**LIR-REF**) suffers from a low monomer conversion as revealed by the low height and small area of the released heat (Fig. 2). Even though t_{max} suggests a reasonably fast curing speed, the flattened and broad curve indicates a delay in monomer conversion.

The addition of the selected divinyl ethers together with the thiol crosslinker leads to a distinctive increase in both peak height and area of the heat enthalpy, which corresponds to higher monomer conversions. This is attributed to the higher number of functional groups and the lower viscosity of the rubber formulations upon the addition of the diluents. Reactive diluents lead to an increase in mobility and facilitate the diffusion of the monomers, which generates an overall higher monomer conversion.[33] In contrast, t_{max} is not significantly changing, which suggests that t_{max} observed for the rubber formulations is mainly related to the reactivity of the photoinitiators.

For a more detailed information on cure kinetics and final monomer conversion, FTIR experiments were performed. FTIR

spectra of the stabilized rubber formulation **LIR-SH-TEG** are shown in Fig. 3 prior to and after UV exposure.

To follow the curing process, the bands of the thiol groups (S–H stretching at 2572 cm^{-1}), carbon double bonds of the divinyl ether (C=C bending at 1641 cm^{-1}) and the main chain carbon double bonds of the isoprene (C=C–H wagging at 840 cm^{-1}) were monitored. In order to calculate the monomer conversion, the area of the characteristic IR absorption bands were integrated and related to a reference band (C=O stretching at 1720 cm^{-1}). The normalized monomer signals were obtained by taking the ratio of the monomer bands to the reference band. Subsequently, the monomer conversion was calculated according to the following eqn (1) where t_0 refers to the initial monomer band and t to the bands at the irradiation time t:

$$\text{Monomer conversion } (\%) = 1 - \frac{\text{normalized peak } (t)}{\text{normalized peak } (t_0)} \times 100 \quad (1)$$

For the reference (**LIR-REF**) system, the methacrylate groups (C=C at 1641 cm^{-1}) are consumed (conversion amounts to 20%) upon UV irradiation. In addition, a slight conversion of the main chain carbon double bonds (C=C at 1666 cm^{-1}) of the isoprene units was observed (Fig. S1 in ESI†). This is in accordance with the broadened peak observed in the photo-DSC experiments, which suggests that the radical induced short chain crosslinking of the isoprene double bonds takes place, albeit very slowly. The low conversion of the main chain C=C bonds of the liquid rubber can be attributed to the low reactivity of non-activated (absence of electron withdrawing groups) carbon double bonds in radical induced addition reactions.[24,34] In addition, previous work revealed that diene-rubbers with alkene groups in the side chain provide a higher reactivity in thiol–ene reactions than *cis*-1,4-poly(isoprene) rubber with C=C groups in the main chain.[35] However, photo-curing of *cis*-1,4-poly(isoprene) rubber either in solid film state or liquid latex state yielded similar crosslink characteristics than sulfur cured systems.[36]

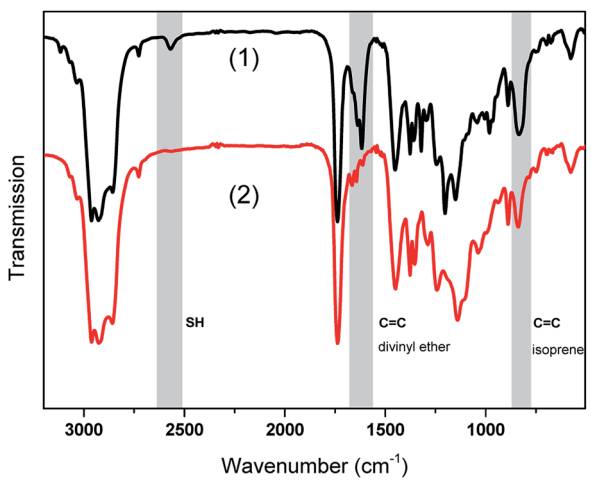

Fig. 3 FTIR spectra of LIR-SH-TEG (1) prior to and (2) after exposure to light (405 nm) for 120 s.

Table 2 Monomer conversion of stabilized formulations after 120 s of irradiation

Formulation	Conversion thiol groups (%)	Conversion vinyl groups (%)	Conversion main chain C=C groups (%)
LIR-REF	—	—	19
LIR-SH-TEG	94	61	55
LIR-SH-DEG	98	53	56
LIR-SH-BD	51	72	65

In the present work, the crosslinking density of the liquid rubber could be significantly increased upon the addition of divinyl ethers as reactive diluents. FTIR data of the stabilized rubber resins reveal that the conversion of the main chain C=C bonds of the isoprene units more than doubled (55–65%) for liquid rubber formulations containing thiol crosslinker and divinyl ether (Fig. S2 in ESI† and Table 2). This result is also in good agreement with literature, where it has already been reported, that reactive diluents have a positive effect on the curing behaviour of liquid isoprene rubber.[24]

Furthermore, FTIR data of the non-stabilized systems (Fig. S3 and Table S1 in ESI†) showed that pyrogallol influences the conversion of the functional groups. Without the addition of a stabilizer, dark reactions already proceed during the mixing of the resin formulation leading to a premature conversion of functional groups and a reduction of the remaining active moieties in the formulation. Thus, thiol and vinyl moieties are already partly consumed before the FTIR experiments have been carried out and a slowing down in the curing kinetics of the non-stabilized resin formulations is observed. In contrast, the addition of Sudan II to the stabilized resin formulations does not significantly affect the cure kinetics (Fig. S4 and Table S1 in ESI†).

However, the cure kinetics of all formulations reveals that the addition of the reactive diluents facilitates a high curing speed. In particular for stabilized systems, the polymerization process is nearly complete after 5 s of light exposure. At longer exposure times, the monomer conversion only slightly increases, which might be due to diffusion limitations of the rubber formulation at higher degree of conversion. Whilst **LIR-SH-DEG** and **LIR-SH-TEG** exhibit similar cure kinetics, **LIR-SH-BD** is characterized by a lower reactivity. Typically, we would expect that reactive diluents with shorter length of the glycol chains show an increased reactivity. However, the opposite behaviour was observed. These results are also corroborated by the photo-DSC data showing the highest photo-reactivity for tri(ethylene glycol) divinylether (**LIR-SH-TEG**), followed by di(ethylene glycol)divinylether (**LIR-SH-DEG**) and butandiol divinylether (**LIR-SH-BD**) as reactive diluents. Previous studies reported an increase in reaction rate for methacrylates with different pendant glycol chains.[34] The higher reactivity was attributed to the mobility of the functional groups, which increases with rising spacer length and makes the functional groups better accessible during the reaction.

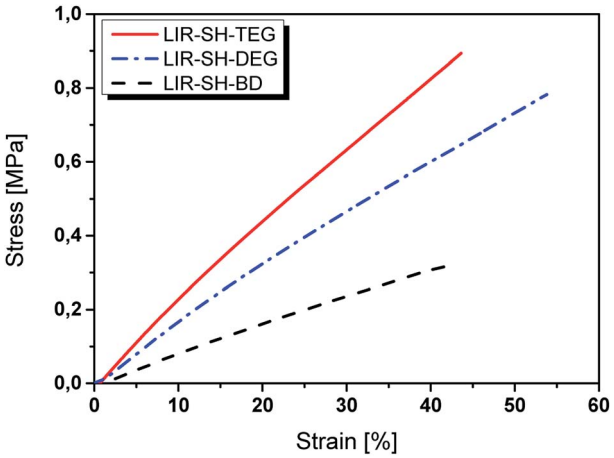

Fig. 4 Tensile properties of rubber formulations containing divinyl ethers as reactive diluents.

Table 3 Tensile results of rubber formulations containing divinyl ethers as reactive diluents

Formulation	Stress (MPa)	Strain (%)	Young's modulus (MPa)
LIR-SH-TEG	0.90 ± 0.12	42 ± 2	2.06 ± 0.42
LIR-SH-DEG	0.78 ± 0.08	54 ± 3	1.45 ± 0.28
LIR-SH-BD	0.32 ± 0.02	42 ± 3	0.78 ± 0.12

In addition, nearly full thiol conversion is observed in **LIR-SH-DEG** and **LIR-SH-TEG**, whilst the thiol conversion amounts to 51% in **LIR-SH-BD**. The results suggest that butandiol divinylether is more prone to side reactions than the other two divinyl ethers. In contrast to cationic photopolymerization, the electron-rich carbon double bonds of divinyl ethers do not undergo homopolymerization in photo-initiated radical polymerizations. However, it has been reported that co-polymerization with other alkenes is highly favoured.[37] Thus, it is assumed that the carbon double bonds of butandiol divinylether in **LIR-SH-BD** preferably undergo a co-polymerization with the main chain C=C double bonds of the rubber instead of participating in thiol–ene click chemistry.

Tensile testing

Tensile testing was carried out to assess the stress–strain behaviour of the liquid rubber formulations, which were photo-crosslinked in silicon moulds. Typically, elastomers show large strain values (several 100%) accompanied with low stress levels. This is due to the long polymeric chains, which show a high degree of flexibility and mobility. By applying an external stress these chains can alter their confirmation facilitating a high elongation of the networks.[16]

The stress–strain behaviour of the photo-cured rubber formulations is displayed in Fig. 4 and the data are summarized in Table 3. The Young's modulus was calculated from the slope of the linear portion of the stress–strain curve. It should be noted that test specimens from **LIR-REF** were very weak and could not be removed from the moulds without destroying the samples. Therefore, no values could be obtained from **LIR-REF**. The poor mechanical properties are mainly related to the low reactivity of the resin formulation, which is associated with a low number of crosslinks.

In contrast, adequate specimens were obtained with the rubber formulations containing the reactive diluents and as an example Fig. 5 illustrates the elasticity of **LIR-SH-DEG** by reversibly twisting the cured specimen by hand. In contrast to technical elastomers, the cured liquid rubber formulations show a rather low elongation at break. This is explained by the low molecular weight of the liquid rubber and the missing physical entanglements, which would significantly contribute to a rubber-like behaviour.

The highest stress and Young's modulus was found for **LIR-SH-TEG** indicating a higher rigidity compared to the other two systems. This behaviour is explained by the higher reactivity of **TEG**, which leads to higher crosslinked networks. Whilst photo-cured **LIR-SH-DEG** exhibits a similar behaviour, albeit at higher strain values, both stress and Young's modulus significantly decrease for photo-cured **LIR-SH-BD**. On the one hand, the low mechanical properties might be related to inhomogeneous network properties due to the high degree of co-polymerization and the associated decrease in crosslink density. On the other hand, photo-cured **LIR-SH-BD** contains a high amount of non-reacted thiols, which are well known to act as lubricants in thiol–ene networks.[38]

3D printing of specimen

In the final step, the rubber formulations were tested according their application in DLP 3D printing. To minimize the effect of light scattering, Sudan II was added to the formulations as an UV-absorber. During the DLP bottom-up printing process several challenges have occurred for the non-stabilized liquid rubber resins. The consistency of the resins was rather sticky with a poor flow behaviour. The resulting challenges included a poor adhesion to the movable platform and difficulties to move fresh layers of resin to the areas, which had to be printed in the next layer. Facing these problems, it is no surprise that recent research has mainly focused on syringe-printed or top-down printed specimen.[19,39]

The non-stabilized rubber formulations showed poor results in the printing process. This was mainly due to the premature

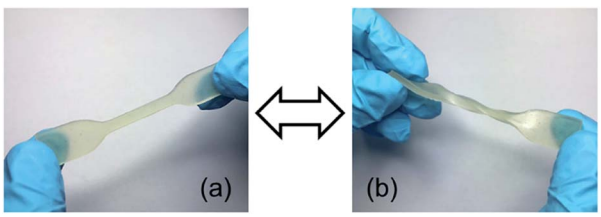

Fig. 5 Reversible twisting of a tensile test specimen from LIR-SH-DEG. The (a) initial test specimen was (b) twisted and could again be recovered to the (a) initial state.

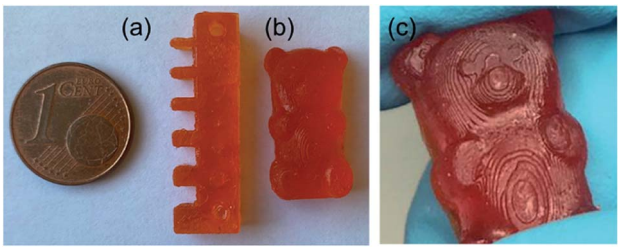

Fig. 6 DLP 3D printed specimen from LIR-SH-TEG: (a) comb and (b) gummy bear. (c) The precise structures of the printed gummy bear are shown in greater detail.

polymerization of the resin in the vat. Gelation occurred during the printing process, which led to either misshaped specimen or a complete stop of the layer-building. However, the addition of pyrogallol enabled the successful printing of well-defined structures. Specimens could be printed for **LIR-SH-TEG** and **LIR-SH-DEG** in a reasonable time.

However, due to the slower network formation of **LIR-SH-BD** the printing time had to be increased significantly. Fig. 6 displays the high resolution of the obtained specimen. The comb demonstrates very well the possible precision of the liquid rubber resins. All spikes (thickness decreases from 3 mm to 0.5 mm) were successfully printed and no accruing of the holes occurred. Thus, the results clearly showed that printing of liquid rubber formulations with bottom-up DLP techniques is feasible with a reasonable precision.

Conclusions

This work demonstrated the successful bottom-up DLP printing of 3D objects with modified liquid diene-rubbers. Photo-induced curing of a methacrylate-functional liquid isoprene rubber was obtained by thiol-click chemistry. Selected low molecular weight divinyl ethers were added as reactive diluents to reduce the viscosity of the liquid rubber from 79 to 1–6 Pa s, which is in a processable range for DLP 3D printing. Along with the viscosity, the reactive diluents significantly improved the photo-reactivity of the modified liquid rubber formulation, which was demonstrated by FTIR and photo-DSC experiments. In particular, the reactivity increased in the order of: **BD** < **DEG** < **TEG**. The results indicate that the photo-reactivity of the divinyl ethers in the thiol–ene reaction increases with rising spacer length of the glycol units. In addition, divinyl ethers with glycol spacer have a higher reactivity than counterparts with alkyl spacer (**DEG** *vs.* **BD**). Besides the reaction rate, the choice of reactive diluent further influences the network structure. Whilst nearly full thiol conversion was observed for **LIR-SH-DEG** and **LIR-SH-TEG** networks, **LIR-SH-BD** systems suffered from a high excess of unreacted thiol. This led to the conclusion that thiol–ene networks are predominately formed in **LIR-SH-DEG** and **LIR-SH-TEG** systems by the well-defined step-growth polymerization. In contrast, copolymerization of **BD** with the main chain C=C of the isoprene units is favoured over thiol–ene reaction in **LIR-SH-BD** formulations.

Since the rubber formulations suffered from premature crosslinking reactions under dark conditions, 0.1 wt% of pyrogallol was added as stabilizer. Rheological measurements revealed that the stability of these rubber formulations was sufficiently high for the subsequent printing process.

Tensile tests revealed that the cured rubber networks suffer from a low strain (<100%) and stress (<1 MPa), which is mainly attributed to the low molecular weight of the liquid rubber and the absence of physical entanglements. In further work, strategies to improve the mechanical properties by network design and printing at higher temperature will be pursued.

However, the bottom-up DLP 3D printing of the rubber formulations could be successfully performed and 3D objects with adequate precision and good resolution were fabricated.

Experimental

Materials and chemicals

Liquid isoprene rubber functionalized with methacrylate groups (17 000 g mol^{-1} with two functional methacrylate groups per oligomer) with the trade name UC-102M has been thankfully received from Kuraray (Chiyoda, Japan). Trimethylolpropane tris(3-mercaptopropionate) (TMPMP) as thiol crosslinker was obtained from Bruno Bock (Marschacht, Germany). Butandiol divinylether (**BD**), tri(ethylene glycol) divinylether (**TEG**) and di(ethylene glycol)divinylether (**DEG**) were from Sigma-Aldrich (St. Louis, USA). The structures of the reactive monomers are shown in Fig. 1a. The photoinitiators phenylbis(2,4,6-trimethylbenzoyl) phosphine oxide (Omnirad 819) and ethyl(2,4,6-trimethylbenzoyl)phenylphosphinate (Omnirad TPO-L) were provided by IGM resins (Waalwijk, The Netherlands). Additionally, to stabilize the reactive systems, pyrogallol from Sigma-Aldrich was added as a radical scavenger. Sudan II, supplied by TCI chemicals (Tokio, Japan), was used as UV-absorber. All chemicals were used as received.

Preparation of rubber formulations for DLP 3D printing

The basic formulation consisted of 100 phr (parts per hundred parts of rubber) UC-102M (liquid rubber) and 30 phr divinylether as reactive diluent. According to the molar mass of the

Table 4 Composition of the liquid rubber formulations

Sample	Type of reactive diluent	Concentration of reactive diluent/phr	Concentration of TMPMP/wt%	Molar ratio C=C/thiol groups	Concentration of pyrogallol/wt%
LIR-REF	—	—	—	—	0.1
LIR-SH-TEG	**TEG**	30	44	1:1	0.1
LIR-SH-DEG	**DEG**	30	57	1:1	0.1
LIR-SH-BD	**BD**	30	64	1:1	0.1

specific divinyl ethers the amount of corresponding thiol was calculated stoichiometrically. In addition, 2 wt% Omnirad 819 and 0.5 wt% Omnirad TPO-L were added as photoinitators. To stabilize the system, 0.1 wt% pyrogallol was placed to the formulations.

For the mixing, a two-axis centrifugal mixer "Vortex" from StateMix (Winnipeg, Canada) was employed. Due to the high viscosity of the liquid rubber it was not possible to dissolve the reactive diluents with a magnetic stirrer. Thus, all components, except the photoinitiators, were homogenized in one step by the Vortex mixer. Subsequently, the now low-viscous mixture was stirred on a magnetic stirrer at 50 °C to ensure a complete incorporation of the stabilizer. In a subsequent step, the photoinitiators were added and the mixture was stirred until all components dissolved into the formulation. The composition of the formulations is summarized in Table 4.

Characterization

The viscosity of the rubber formulations was determined on a Modular Compact Rheometer MCR 102 from Anton Paar (Graz, Austria) with a CP60-0.5/TI cone (60 mm diameter and 0.5° opening angle). Each measurement was performed with 1 mL of sample at 25 °C and 300 s^{-1} shear rate.

For the photo-DSC measurements samples of 8 ± 0.05 mg were weighed in aluminium crucibles, which were analysed in a NETZSCH Photo-DSC 204 F1 Phoenix (Selb, Germany). The measurements were performed under nitrogen flow (20 mL min^{-1}) at 50 °C. As light source an Omnicure s2000 UV-Lamp was used at 1 W cm^{-1}.

FTIR measurements were performed on a VERTEX 70 (Bruker, Billerica, USA) in transmission mode to monitor the cure kinetics. 1 μL of the rubber formulation was placed on a Si-wafer and illuminated for a defined time with an Omnicure s1000 (Lumen Dynamics, Mississauga, USA) at 100% intensity (436 mW cm^{-2}) with a 5 cm distance between sample surface and light source.

Tensile testing was performed according to ISO 37-S2 using a Z001 from Zwick Roell (Ulm, Germany) with a crosshead speed of 200 mm min^{-1}. Measurements were carried out at room temperature. For sample preparation, silicon moulds with dimensions of 2 × 12.5 × 75 mm were prepared. The UV-curable rubber formulation was filled in the moulds and cured with a ND24 (Ostfildern, Germany) LED curing device at 385 nm for 10 min (124 mW cm^{-2}). After curing, the samples were demoulded and washed with isopropanol.

3D Printing

To minimize the effect of light scattering, 0.01 wt% Sudan II was added to the rubber formulations prior to the 3D printing experiments. 3D printing was carried out *via* digital light processing (DLP) technique using a mUVe 3D test printer (Grand Rapids, USA). As a light source, a ViewSonic projector (1920 × 1080 pixel) was placed underneath a transparent resin container. During the printing process, the resin is illuminated and the cured sample sticks to a moving platform above the container (Fig. 1b). The platform moves in vertical direction after each illumination step and stops at a defined height. Each layer was set to 100 μm and illuminated for 70 s.

The CAD drawings have been thankfully received from the Luxinergy GmbH (comb) and jakejake from http://thingiverse.com (gummy bear).

Conflicts of interest

There are no conflicts to declare.

Acknowledgements

The research work was performed within the COMET-Module project "Chemitecture" (project-no.: 21647048) at the Polymer Competence Center Leoben GmbH (PCCL, Austria) within the framework of the COMET-program of the Federal Ministry for Transport, Innovation and Technology and the Federal Ministry for Digital and Economic Affairs with contributions by Montanuniversitaet Leoben (Chair of Chemistry of Polymeric Materials). The PCCL is funded by the Austrian Government and the State Governments of Styria, Lower Austria and Upper Austria. Further thanks goes to Klara Kaml, Nils Marchler and Nico Dormann from the HTL Kapfenberg (Austria), who supported the lab work during their internship.

References

1 (*a*) M. Park, J. Park and U. Jeong, *Nano Today*, 2014, **9**, 244–260; (*b*) W. Balasooriya, B. Schrittesser, S. Karunakaran, S. Schlögl, G. Pinter, T. Schwarz and Z. Kadar, *Macromol. Symp.*, 2017, **373**, 1600093; (*c*) C. Graf, J. Hitzbleck, T. Feller, K. Clauberg, J. Wagner, J. Krause and J. Maas, *J. Intell. Mater. Syst. Struct.*, 2013, **25**, 951–966.

2 S. A. Morin, R. F. Shepherd, S. W. Kwok, A. A. Stokes, A. Nemiroski and G. M. Whitesides, *Science*, 2012, **337**, 828–832.

3 (*a*) C. Pang, G.-Y. Lee, T.-i. Kim, S. M. Kim, H. N. Kim, S.-H. Ahn and K.-Y. Suh, *Nat. Mater.*, 2012, **11**, 795–801; (*b*) K. Cherenack, C. Zysset, T. Kinkeldei, N. Münzenrieder and G. Tröster, *Adv. Mater.*, 2010, **22**, 5178–5182.

4 (*a*) D. B. Kolesky, K. A. Homan, M. A. Skylar-Scott and J. A. Lewis, *Proc. Natl. Acad. Sci. U. S. A.*, 2016, **113**, 3179–3184; (*b*) T. J. Hinton, A. Hudson, K. Pusch, A. Lee and A. W. Feinberg, *ACS Biomater. Sci. Eng.*, 2016, **2**, 1781–1786.

5 J. T. Muth, D. M. Vogt, R. L. Truby, Y. Mengüç, D. B. Kolesky, R. J. Wood and J. A. Lewis, *Adv. Mater.*, 2014, **26**, 6307–6312.

6 (*a*) A. A. S. Bhagat, P. Jothimuthu and I. Papautsky, *Lab Chip*, 2007, **7**, 1192–1197; (*b*) M. Sangermano, S. Marchi, P. Meier and X. Kornmann, *J. Appl. Polym. Sci.*, 2012, **1**, 1521–1526.

7 D. A. Porter, A. L. Cohen, P. S. Krueger and D. Y. Son, *3D Printing and Additive Manufacturing*, 2018, **5**, 73–86.

8 B. C. M. Murray, B. N. Peele, P. Xu, J. Spjut, O. Shapira, D. Luebke and R. F. Shepherd, *2018 IEEE International Conference on Soft Robotics (RoboSoft)*, 2018, pp. 264-269.

9 S.-G. Woo, I. H. Lee and K.-C. Lee, *J. Mech. Sci. Technol.*, 2015, **29**, 3905–3909.

10 W. Su, S. A. Nauroze, B. Ryan and M. M. Tentzeris, *Dig. - IEEE MTT-S Int. Microw. Symp.*, 2017, 1579–1582.
11 B. N. Peele, T. J. Wallin, H. Zhao and R. F. Shepherd, *Bioinspiration Biomimetics*, 2015, **10**, 55003.
12 D. K. Patel, A. H. Sakhaei, M. Layani, B. Zhang, Q. Ge and S. Magdassi, *Adv. Mater.*, 2017, **29**, 1–7.
13 B. C. Gross, J. L. Erkal, S. Y. Lockwood, C. Chen and D. M. Spence, *Anal. Chem.*, 2014, **86**, 3240–3253.
14 S. C. Ligon, R. Liska, J. Stampfl, M. Gurr and R. Mülhaupt, *Chem. Rev.*, 2017, **117**, 10212–10290.
15 J. Herzberger, J. M. Sirrine, C. B. Williams and T. E. Long, *Prog. Polym. Sci.*, 2019, **97**, 101144.
16 J. G. Drobny, *Handbook of Thermoplastic Elastomers*, William Andrew Publishing, Norwichh, NY, 2014.
17 S. Schlögl, M.-L. Trutschel, W. Chassé, I. Letofsky-Papst, R. Schaller, A. Holzner, G. Riess, W. Kern and K. Saalwächter, *Polymer*, 2014, **55**, 5584–5595.
18 M. Akiba and A. S. Hashim, *Prog. Polym. Sci.*, 1997, **22**, 475–521.
19 P. J. Scott, V. Meenakshisundaram, N. A. Chartrain, J. M. Sirrine, C. B. Williams and T. E. Long, *ACS Appl. Polym. Mater.*, 2019, **1**, 684–690.
20 M. Bragaglia, F. R. Lamastra, V. Cherubini and F. Nanni, *Express Polym. Lett.*, 2020, **14**, 576–582.
21 C. Decker, H. Le Xuan and T. N. Thi Viet, *J. Polym. Sci., Part A: Polym. Chem.*, 1995, **33**, 2759–2772.
22 C. Decker, *Surf. Coating. Int. B Coating. Trans.*, 2005, **88**, 9–17.
23 H. L. E. Xuan and C. Decker, *J. Polym. Sci., Part A: Polym. Chem.*, 1993, 769–780.
24 P. Phinyocheep and S. Duangthong, *J. Appl. Polym. Sci.*, 2000, **78**, 1478–1485.
25 P. Taylor, L. S. Andrews and J. J. Clary, *J. Toxicol. Environ. Health*, 2015, 37–41.
26 A. Faldi and M. Tirrell, *Macromolecules*, 1994, 4184–4192.
27 C. Hinczewski, S. Corbel and T. Chartie, *J. Eur. Ceram. Soc.*, 1998, **18**(6), 583–590.
28 (*a*) G. Kühne, J. S. Diesen and E. Klemm, *Angew. Makromol. Chem.*, 1996, **242**, 139–145; (*b*) E. Klemm, S. Sensfuß, U. Holfter and H. J. Flammersheim, *Angew. Makromol. Chem.*, 1993, **212**, 121–127.
29 V. Preedy, *Coffee in Health and Disease Prevention*, Academic Press, London, 2014.
30 P. Esfandiari, S. C. Ligon, J. J. Lagref, R. Frantz, Z. Cherkaoui and R. Liska, *J. Polym. Sci., Part A: Polym. Chem.*, 2013, **51**(20), 4261–4266.
31 M. Edler, F. H. Mostegel, M. Roth, A. Oesterreicher, S. Kappaun and T. Griesser, *J. Appl. Polym.Sci.*, 2017, 44934.
32 A. Mautner, X. Qin, H. Wutzel, S. C. Ligon, B. Kapeller, D. Moser, G. Russmueller, J. Stampfl and R. Liska, *J. Polym. Sci., Part A: Polym. Chem.*, 2013, **51**, 203–212.
33 L. G. Lovell, J. W. Stansbury, D. C. Syrpes and C. N. Bowman, *Macromolecules*, 1999, **32**, 3913–3921.
34 A. B. Scranton, C. N. Bowman, J. Klier and N. A. Peppas, 1992, **33**, 1683–1689.
35 (*a*) D. Lenko, S. Schlögl, A. Temel, R. Schaller, A. Holzner and W. Kern, *J. Appl. Polym. Sci.*, 2013, **129**, 2735–2743; (*b*) D. Lenko, S. Schlögl, A. Temel, R. Schaller, A. Holzner and W. Kern, *J. Appl. Polym. Sci.*, 2013, **129**, 2735–2743; (*c*) S. Schlögl, A. Temel, R. Schaller, A. Holzner and W. Kern, *J. Appl. Polym. Sci.*, 2012, **124**, 3478–3486; (*d*) S. Schlögl, M.-L. Trutschel, W. Chassé, I. Letofsky-Papst, R. Schaller, A. Holzner, G. Riess, W. Kern and K. Saalwächter, *Polymer*, 2014, **55**, 5584–5595.
36 (*a*) S. Schlögl, M.-L. Trutschel, W. Chassé, G. Riess and K. Saalwächter, *Macromolecules*, 2014, **47**, 2759–2773; (*b*) W. Chassé, S. Schlögl, G. Riess and K. Saalwächter, *Soft Matter*, 2013, **9**, 6943–6954.
37 C. Decker and D. Decker, *J. Macromol. Sci., Part A: Pure Appl.Chem.*, 1997, **34**, 605–625.
38 S. Mongkhontreerat, K. Öberg, L. Erixon, P. Löwenhielm, A. Hult and M. Malkoch, *J. Mater. Chem. A*, 2013, **1**, 13732.
39 X. Kuang, K. Chen, C. K. Dunn, J. Wu, V. C. F. Li and H. J. Qi, *ACS Appl. Mater. Interfaces*, 2018, **10**, 7381–7388.

